

Scanning electrochemical microscopy (SECM) study of superoxide generation and its reactivity with 1,4-dihydropyridines

S. Bollo, P. Jara-Ulloa, S. Finger, L.J. Núñez-Vergara, J.A. Squella *

Bioelectrochemistry Laboratory, Chemical and Pharmaceutical Sciences Faculty, University of Chile, P.O. Box 233, Olivos, Santiago 1 1007, Chile

Abstract

A scanning electrochemical microscope (SECM), in the tip generation substrate collection and feedback modes, was used in a method to characterize the electrode mechanism of the $O_2/O_2^{\bullet -}$ couple in dimethylsulphoxide (DMSO) containing 0.1 M tetrabutylammonium perchlorate (TBAP) as the supporting electrolyte. Also the quantification of the interaction between $O_2^{\bullet -}$ and different 1,4-dihydropyridine compounds is reported.

The SECM results demonstrated that the $O_2/O_2^{\bullet -}$ couple follows an E mechanism, in contrast with the EC_2 mechanism (DISP 2) that was previously reported by cyclic voltammetry. This result implies that in the time scale of SECM measurements there is no time for a homogeneous chemical reaction to be coupled to the electron transfer, i.e., the superoxide is a stable radical. Also we have determined the heterogeneous standard rate constant, k^0 of the quasi-reversible reduction of oxygen to superoxide anion.

Taking advantage of the fact that the superoxide suffers no chemical decay during the SECM experiment, a method to obtain the direct interaction of different 1,4-dihydropyridine molecules with superoxide was developed. The study revealed that all the 1,4-DHPs scavenged superoxide with sufficiently high interaction constants ($\sim 10^5 M^{-1} s^{-1}$). No significant difference between the different molecules was found.

This paper shows that the SECM feedback mode is a sensitive technique, giving an accurate determination of the homogeneous interaction constant and allowing the determination of faster rate constants than those found from cyclic voltammetry.

Keywords: Superoxide; SECM; 1,4-Dihydropyridines

1. Introduction

The study of biological radicals is a topic of increasing interest in the scientific literature due to its importance in different processes involved in human life. The superoxide radical anion ($O_2^{\bullet -}$) is one of the most important radicals in biology, because it is the starting point for the formation of the well-known reactive oxygen species (ROS). $O_2^{\bullet -}$ is implicated in several harmful biological processes, such as lipid peroxidation and protein denaturation. The reactivity of $O_2^{\bullet -}$ in an aqueous med-

ium is quite different from that in aprotic media. In an aqueous medium, $O_2^{\bullet -}$ disproportionates spontaneously into hydrogen peroxide and molecular oxygen, whereas in an aprotic medium $O_2^{\bullet -}$ is stable and can show reactivity in several forms, e.g., as an electrogenerated base, nucleophile, reductant and oxidant.

Although the electrochemical reduction of oxygen to $O_2^{\bullet -}$ in aprotic solvents has been known for several decades [1–4] there is still interest in learning more about the electrochemistry of this radical. Recently, the use of cyclic voltammetry for the generation, detection and reactivity of $O_2^{\bullet -}$ towards different compounds has been reported at different electrodes [5–9]. In this field, we have described the reaction between $O_2^{\bullet -}$ and a series of Hantzsch 1,4-dihydropyridines of pharmacological

* Corresponding author. Tel.: +56 2 678 29 28/2927; fax: +56 2 737 12 418/1241.

E-mail address: asquella@ciq.uchile.cl (J.A. Squella).

significance, revealing that electrogenerated $O_2^{\bullet-}$ quantitatively oxidizes dihydropyridine derivatives to produce the corresponding aromatized pyridine derivatives [10]. Up-to-date electrochemical studies of $O_2^{\bullet-}$ have been carried out using only cyclic voltammetric measurements, but the extension of these studies by introducing scanning electrochemical microscopy (SECM) measurements as a new alternative approach is our current challenge. SECM has been described as useful in studying the kinetics and mechanism of coupled reactions associated with electrode processes [11–15]. The use of SECM eliminated many typical sources of experimental errors, e.g., the effects of the resistive potential drop in solution and the charging current and enabled analytical measurements to be performed in the interfacial region [16]. On the other hand, because SECM measurements can be made under steady-state conditions, short-time measurements are not needed, and contributions by possible adsorbed electroactive species are avoided, providing a great advantage in the study of free radicals of biological significance. Finally, the steady-state TG/SC mode, in particular, appears to be attractive for measuring fast chemical reactions with rate constants of the order of $4 \times 10^8 \text{ M}^{-1} \text{ s}^{-1}$, which is in excess of those achievable via cyclic voltammetry, where it is not possible to study rate constants higher than $2 \times 10^4 \text{ M}^{-1} \text{ s}^{-1}$.

Consequently, considering that generally free radicals formed by an electron transfer first step decay by a first or second order chemical reaction, the use of this novel technique to the study of $O_2^{\bullet-}$ would be a very good alternative. To the best of our knowledge there are no reports about the use of SECM to characterize the electrochemical behavior of $O_2^{\bullet-}$ in solution. In this work, we employed SECM TG/SC and the feedback mode in non-aqueous aprotic media to study the $O_2/O_2^{\bullet-}$ couple and the interaction between superoxide and a series of well-known 1,4-dihydropyridine-calcium antagonist drugs (Fig. 1).

2. Experimental

2.1. Reagents

The aprotic solvent, dimethylsulfoxide (DMSO), used in the electrochemical experiments was purchased from Merck and was dried with 3 Å molecular sieves. All the electrochemical experiments were carried out in an aprotic medium (100% DMSO) with 0.1 M tetrabutylammonium perchlorate (TBAP) as the supporting electrolyte (Fluka), ferrocene and *N,N,N',N'*-tetramethyl-1,4-phenylenediamine (TMPD), (all from

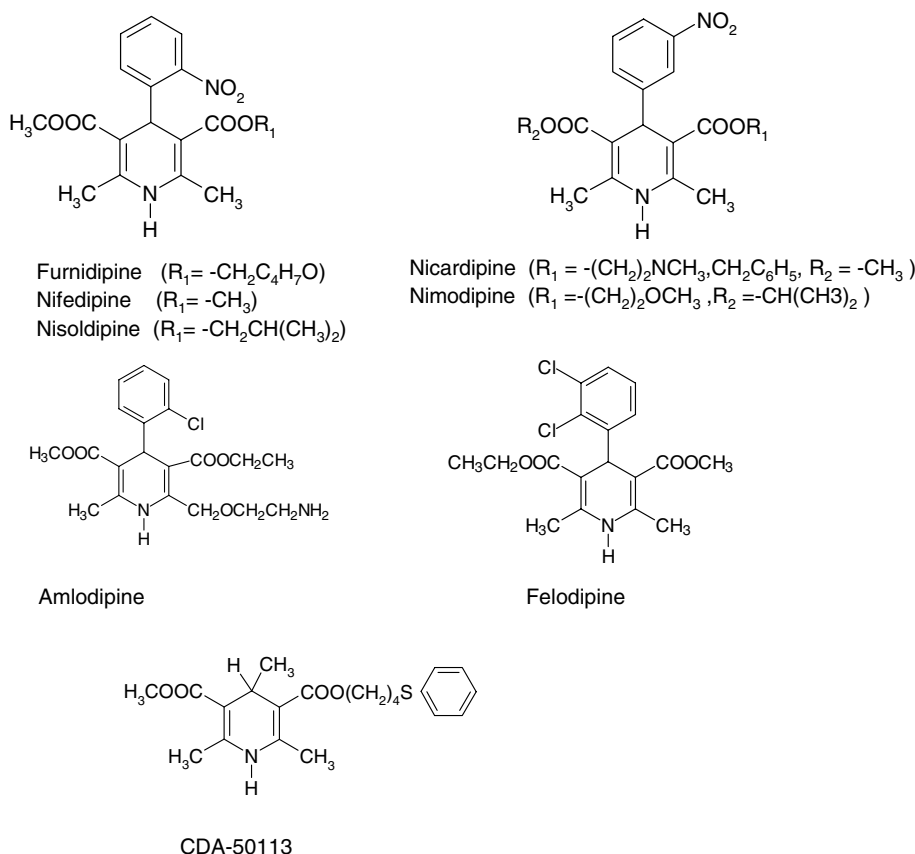


Fig. 1. Chemical structures of 1,4-DHP derivatives.

Aldrich Chemical Co., Inc., Milwaukee, WI) were used without further purification. Oxygen (99.8% pure) and nitrogen (99.9% pure) were purchased from AGA (Santiago, Chile).

2.2. Apparatus

The SECM and cyclic voltammetric experiments were carried out with a CHI 900 setup (CH Instruments Inc., USA). A 10 μm diameter carbon fiber electrode served as the SECM tip. A 100 μm diameter glassy carbon electrode was used as the SECM substrate. A 0.5 mm diameter Pt wire and an Ag|AgCl|KCl(sat.) electrode were used as the counter and reference electrodes, respectively.

Before each experiment the tip and the substrate were polished with 0.3 and 0.05 μm alumina, and then rinsed with water. All the experiments were carried out at controlled temperature ($25 \pm 2^\circ\text{C}$).

For measurements in oxygen media, O_2 gas was bubbled directly into the cell in order to obtain an oxygen solution, and during the measurement, O_2 gas was flushed over the cell solution. Two flow meters (Cole Palmer 316SS) for oxygen and nitrogen, respectively, equipped with needle valves were used. Knowing the oxygen solubility in DMSO containing 0.1 M TEAP [17] and by establishing the oxygen and nitrogen flow rates, it was possible to determine the concentration of oxygen in the measurement cell [18].

2.3. SECM experiments (Fig. 2)

The feedback mode is the main quantitative operation mode of SECM. When the tip is far from the substrate

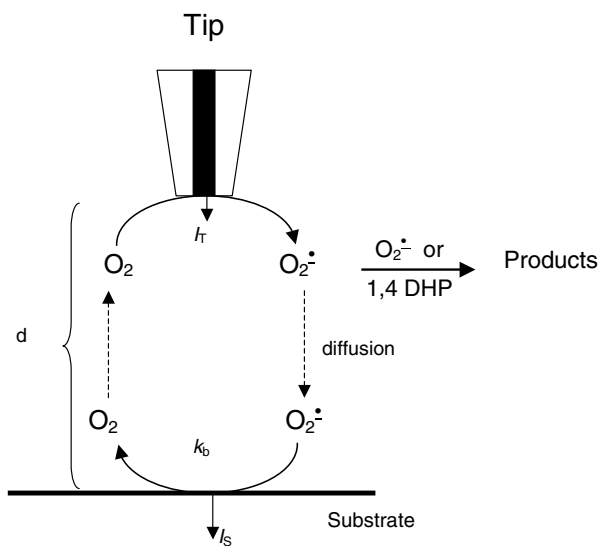


Fig. 2. SECM array scheme illustrating the tip generation/substrate collection mode for superoxide generation and its reactivity.

and a potential that permits the redox process to occur is applied, the steady-state current, $I_{T,\infty}$, is given by

$$I_{T,\infty} = 4nFDca \quad (1)$$

where F is the Faraday constant, n is the number of electrons transferred in the tip reaction, D is the diffusion coefficient of electroactive species, c is the bulk concentration of the species and a is the tip radius. When the substrate is conductive, a higher tip current is observed ($I_T > I_{T,\infty}$) when the tip is closer to the substrate and then a positive feedback takes place. When the substrate is insulating, a lower tip current is observed ($I_T < I_{T,\infty}$) when the tip is closer to the substrate, meaning that a negative feedback takes place.

SECM results are presented in the dimensionless form $i_T(L)$ vs. L , where the experimental feedback current was normalized by the steady-state current, $I_{T,\infty}$, i.e., $i_T(L) = I_T/I_{T,\infty}$ and L is da . The absolute distance d is obtained from the diffusion-controlled steady-state current–distance curve according to the analytical approximations for SECM with a disk-shaped tip [19]:

$$i_T(L) = I_T/I_{T,\infty} = 0.68 + 0.78377/L + 0.3315 \exp(-1.0672/L). \quad (2)$$

The heterogeneous rate constant k^0 for the ET reaction can be extracted from the fitting SECM experimental current (I_T)–distance (d) curve (or approach curve) to the theoretical value. The experimental I_T – d curve was recorded while the tip was approaching the substrate surface at a speed of $0.1 \mu\text{m s}^{-1}$. A sufficiently negative potential (-1.1 V) was applied to the tip so that the oxygen was reduced at a diffusion-limited rate. For each current–distance curve, the substrate was biased at different potentials, between 0.2 and -0.7 V prior to and during the acquisition of data. After the experimental data were acquired, a theoretical fitting equations was used [20–25], and the best fit of K_b was obtained, where K_b corresponds to the dimensionless kinetic parameter ($K_b = ak_{b,s}/D$). The rate constant for oxidation ($k_{b,s}$) at the substrate is given by the well-known Butler–Volmer equation:

$$K_b = (ak^0/D) \exp[(1 - \alpha)nF(E - E^0)/RT], \quad (3)$$

where k^0 is the standard rate constant, E is the electrode potential, E^0 is the formal potential (-0.72 V), α is the transfer coefficient, n is the number of electrons transferred per redox event, F is the Faraday constant, R the gas constant, T is the absolute temperature, D is the diffusion coefficient of the electroactive species and a is the tip radius. The subscripts indicate the substrate process. Thus, a plot of $\text{Ln } K_{b,s}$ vs. $(E_S - E^0)$ will give α and k^0 .

To calculate the interaction constant between the 1,4-dihydropyridine derivatives, k_i the normalized tip

(feedback) current as a function of the gap spacing (normalized by the tip radius, a) d/a , at three different 1,4-DHP concentrations, was fitted to the theoretical curves for an EC mechanism developed for a second-order homogeneous chemical reaction [12]. With the best fit for each concentration we estimate a dimensionless rate constant, $K(K = k_i a^2 c/D)$ and then the corresponding k_i .

3. Results and discussion

3.1. SECM characterization of the $O_2/O_2^{\cdot-}$ redox couple mechanism

The SECM technique was applied to study the electroreductive behavior of O_2 . The $O_2/O_2^{\cdot-}$ redox couple on the HMDE in DMSO aprotic media was previously studied by cyclic voltammetry [26]. That study reported that oxygen reduction followed an EC mechanism with the superoxide disproportionation reaction as the chemical step as follows:



The disproportionation constant (k_{2c}) value obtained by cyclic voltammetry in the previous work was $(4.08 \pm 0.21) \times 10^3 \text{ M}^{-1} \text{ s}^{-1}$ [26].

A $10 \mu\text{m}$ carbon fiber tip electrode and a $100 \mu\text{m}$ glassy carbon substrate electrode were used in the SECM experiments. The experiments were carried out in DMSO and at the beginning; ferrocene was used as a calibration mediator. In Fig. 3, the tip and substrate voltammetry at large tip–substrate separations shows the reduction of oxygen to form $O_2^{\cdot-}$ at about -0.85 V . The steady state current yielded a value of $D = (2.23 \pm 0.08) \times 10^{-5} \text{ cm}^2 \text{ s}^{-1}$ (obtained from Eq. (1)) which is close to that of $D = 7.49 \times 10^{-5} \text{ cm}^2 \text{ s}^{-1}$ re-

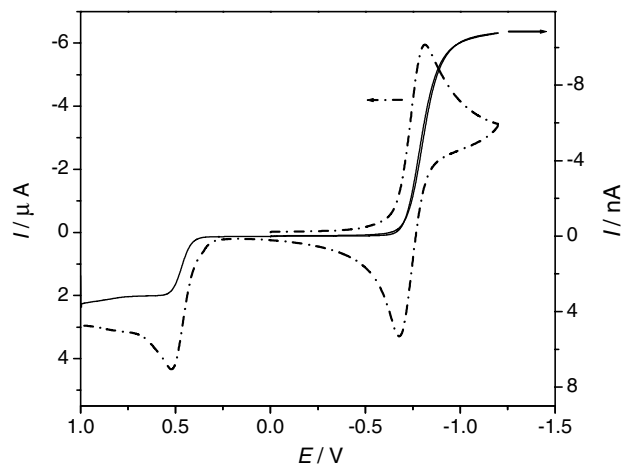


Fig. 3. Cyclic voltammogram at the tip (entire line) and at the substrate (dashed line) at a large tip–substrate separation. Experimental parameters are: $[O_2] = 2.13 \text{ mM}$, $[Fc] = 3 \text{ mM}$, scan rate 100 mV/s .

ported in the literature [27]. Also in Fig. 3 the electrooxidation of ferrocene occurring at about 0.5 V is shown.

Data were collected using the SECM in the tip generation/substrate collection mode (TG/SC). According to the previously reported mechanism, in this mode of operation, the $O_2^{\cdot-}$ electrogenerated at a microelectrode tip can follow two paths: oxidation at the substrate electrode or homogeneous reaction in the gap to form an electroinactive species prior to reaching the substrate. The oxygen, which is regenerated at the substrate, is fed back to the tip. The measured anodic current at the substrate (collection current) and the cathodic tip current (feedback current) are functions of both the electrode separation, d and the homogeneous reaction rate in the gap, k_{2c} . The SECM reaction scheme for the $O_2/O_2^{\cdot-}$ redox couple is illustrated in Fig. 2.

In Fig. 4, typical tip and substrate current responses at tip–substrate separations of infinite and $\sim 10 \mu\text{m}$ are

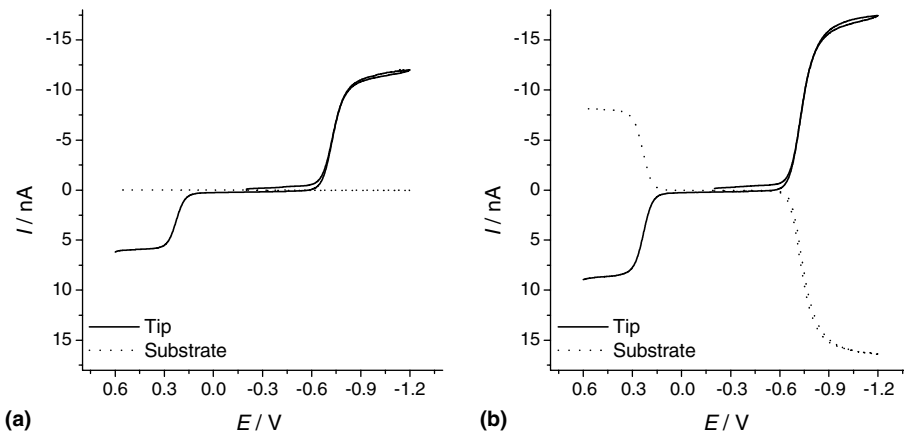


Fig. 4. SECM cyclic voltammograms of oxygen and ferrocene at a tip substrate separation of (a) infinity and (b) $10 \mu\text{m}$ in the TG/SC mode, where the tip is scanned to the first reduction of O_2 and then to the oxidation of ferrocene at a scan rate of 50 mV/s with the substrate potential, E_s held at 0.0 V . Experimental parameters are: $[O_2] = 2.13 \text{ mM}$, $[Fc] = 3.0 \text{ mM}$.

shown. A 50 mV/s scan rate was applied to the tip, which is the generator electrode (TG), while the substrate acts as the collector (SC) and is held at 0.0 V (see Fig. 2). In this figure, it is possible to observe that when the electrodes are at a large tip–substrate separation ($d > 20a$, infinite), the substrate does not collect current due to the oxidation of the superoxide or reduction of Fc^+ , both species being generated at the tip (Fig. 4(a)). On the other hand, when the electrodes are close (e.g., $d \sim 10 \mu\text{m}$) a very high collection efficiency was found for the O_2^- generated and also for the Fc/Fc^+ couple (Fig. 4(b)).

Analyzing the feedback tip current–distance curves, obtained from the TG/SC experiments at different concentrations of ferrocene as the calibration mediator, a change in the behavior of the O_2/O_2^- redox couple was observed at higher ferrocene concentrations (Fig. 5(a)). According to these results, an apparent interaction between ferrocene and the superoxide radical anion is occurring in the gap between the two electrodes.

In previous work [13], an interaction for the mediator ferrocene with ArO^\cdot generated by the oxidation of nitrophenolate (ArO^-) was described. The reported reaction is a redox reaction, since the ArO^\cdot electrogenerated is a good oxidant. However, the direct reactivity between Fe^{2+} or ferrocene and O_2^- is a totally new finding; consequently further studies are necessary to determine the mechanism of this interaction. However, in SECM experiments the mediators should not interfere with the reaction being measured, therefore a new mediator should be selected. In Fig. 5(b), the feedback tip current–distance curves for the O_2/O_2^- redox couple in the presence of TMPD, which is oxidized at about 0.25 V, are shown. As no evidence of any interaction between the molecules was observed, TMPD was selected as a more suitable mediator for this system, and then all further experiments were conducted with this redox mediator.

Representative cyclic voltammograms (CV) illustrating the SECM tip current for oxygen with TMPD as an internal reference, are shown in Fig. 6(a). CVs of both species at six tip–substrate separations, $d \rightarrow \infty$ (dotted line) and $1 < d < 10 \mu\text{m}$ (solid lines) are shown. As expected for a stable couple, the tip current for TMPD increases at small separation due to positive feedback from the substrate. For the O_2/O_2^- redox couple, the SECM response was not as expected for a couple that involves a follow-up chemical reaction, i.e., the tip current does not diminish with respect to the diffusion-controlled feedback current (TMPD), even at high oxygen concentrations. The normalized tip experimental current for three different concentrations shows similar behavior to that predicted for a simple diffusion-controlled feedback, deduced from the experiments of TMPD oxidation (Fig. 6(b)). The same behavior was observed when the current efficiency (I_S/I_T) was analyzed, i.e., a 100% substrate collection for three different O_2 concentrations, furthermore there are no differences in the behavior with TMPD (inset Fig. 6(b)).

According to the diagnostic criteria, no coupled homogeneous chemical reactions, on the time scale of SECM measurements are observed; therefore, we can conclude that the mechanism for the electrogenerated superoxide is a simple E mechanism. This result is surprisingly different from that previously described by cyclic voltammetry. Probably this difference is a consequence of the fact that SECM and CV have different scale times. Bard and co-workers [11–15] studied different mechanisms (E_rC_1 , E_rC_2 , ECE and DISP 1), developing the current SECM theories in order to calculate heterogeneous and homogeneous constants. In all cases a good agreement between the calculated homogeneous chemical constant, k_c using SECM and other techniques was obtained. On the other hand, we have also reported a good correlation between cyclic voltammetric and SECM determination of chemical rate constants for

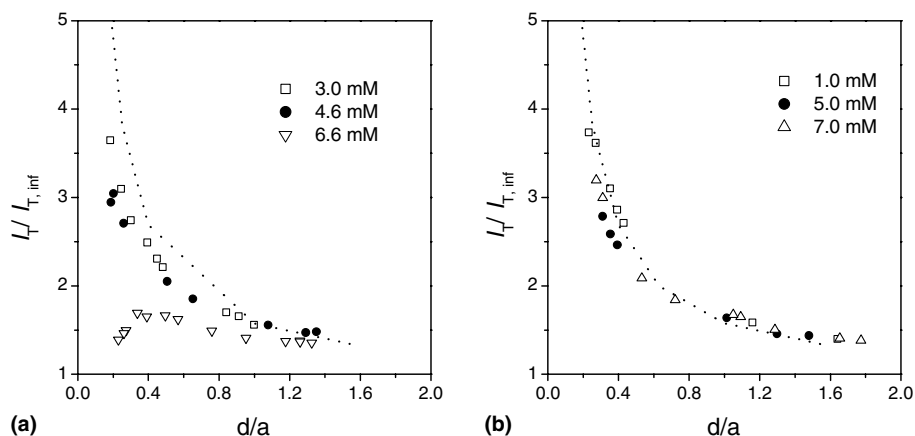


Fig. 5. Normalized tip (feedback) current–distance behavior for $[\text{O}_2]$ at different concentrations of (a) ferrocene and (b) TMPD.

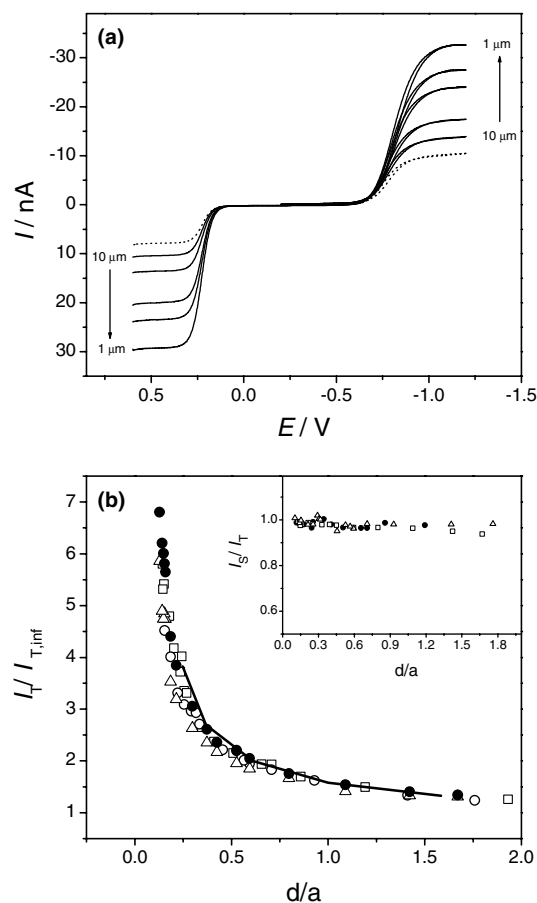


Fig. 6. (a) Representative SECM cyclic voltammograms of oxygen and TMPD taken in feedback mode. Tip scan rate = 50 mV/s. Substrate potential = 0.0 V. Experimental parameters are $[O_2] = 2.13$ mM and $[TMPD] = 5$ mM. Cyclic voltammograms are shown for a very large tip-substrate separation (dotted line) and $d < 10$ μm separation (solid lines). (b) Normalized tip (feedback) current-distance curves for $[O_2] = 2.1$ mM (\circ), 1.03 (\square) and 0.52 mM (\triangle). The simple diffusion-controlled feedback behavior, deduced from experiments with TMPD oxidation (\bullet) and the theoretical approach curve for a perfect conducting substrate (solid line) are also shown. Inset: SECM collection efficiencies (I_S/I_T)-distance curves for $[O_2] = 2.1$ mM (\circ), 1.03 (\square) and 0.52 mM (\triangle).

two different nitrocompounds which follow an $E_T C_{2i}$ mechanism [28].

3.2. Measurements of the heterogeneous rate constant k^0

From previous CV studies [29], it is well known that the oxygen reduction to O_2^- corresponds to a diffusion-limited, quasi-reversible one-electron transfer. Now using the SECM we have studied the effective heterogeneous rate constant k^0 fitting the SECM experimental current (I_T)-distance (d) curve to the theoretical curve [20]. Fig. 7 shows the experimental I_T - d curves fitted with the theoretical curve under different conditions of applied substrate potentials. While the tip approaches the substrate, the tip current response to distance is dependent only upon the k_b value of the reverse reaction on

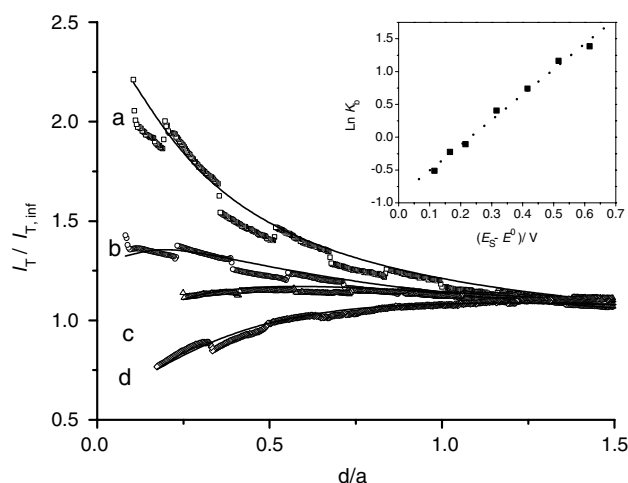


Fig. 7. SECM approach curves obtained with a 12.2 μm diameter carbon fiber, with the tip ($E_{\text{appl}} = -1.1$ V) on the glassy carbon substrate biased at different potentials (a) -0.1 V, (b) -0.3 V, (c) -0.4 V and (d) -0.5 V. The different solid lines represent the theoretical curves fitted with experimental data. Inset: Dependence of the $\text{Ln } K_b$ on $(E_S - E^0).E^0$ for the O_2/O_2^- couple = -0.72 V. k_b values 0.46 (curve a), 0.24 (curve b), 0.172 (curve c) and 0.103 (curve d). The irregularities observed are small discontinuities due to an artifact caused by the piezo click of the z-motors.

the substrate (Fig. 2). The rate constant for oxidation (k_b) at the substrate is given by the Butler-Volmer equation (see Section 2), then an increase in the overpotential (while keeping the values of the other parameters constant) leads to a higher feedback current (curve a, Fig. 7); i.e., at sufficiently high overpotentials, the substrate behaves like a conductor with diffusion-controlled feedback. On the other hand, when the overpotential is low (curves d, Fig. 7), the rate of the feedback process at the substrate is negligible; the substrate behaves like an insulator. The inset to Fig. 7 shows a plot of $\text{Ln } K_b$ vs. the substrate potential. From linear regression of three independent experiments, the k^0 was 0.046 ± 0.006 cm s^{-1} . This k^0 value is in accord with a previous value determined by CV of 0.093 ± 0.004 cm s^{-1} [29]. On the other hand, the α value determined using the same methodology was 0.9.

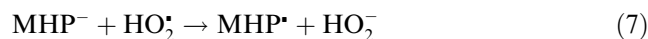
3.3. Interaction between superoxide and 1,4-dihydropyridines

As the superoxide is a radical species that is of special interest in biological systems, since it is one of the most abundant radicals in living cells, it is a real challenge to find a simple method that permits the study of its reactivity towards different molecules, in order to find efficient scavengers. As the mechanism determined for the O_2/O_2^- redox couple by SECM is an E mechanism, this technique is attractive in developing studies of this kind, in view of the fact that there are no coupled reactions that can complicate the reactivity studies.

Thus, in order to study the interaction of different 1,4-dihydropyridines with superoxide, we have examined the effect of adding these compounds on the SECM response of the $O_2/O_2^{\bullet-}$ couple. Fig. 8 shows the normalized tip (feedback) current–distance curves for $[O_2] = 2.1$ mM (\circ), in the presence of different concentrations of nicardipine. In this figure, it is possible to observe that with the addition of nicardipine, the normalized tip (feedback) current of O_2 decreases. These data suggest that nicardipine reacts with $O_2^{\bullet-}$; that is, it scavenges $O_2^{\bullet-}$, which cannot reach the substrate to regenerate oxygen, in a concentration-dependent way. This reaction between superoxide and other 1,4-dihydropyridine derivatives, such as nisoldipine, was previously described [26], it being suggested that the first step in the chemical reaction between superoxide and these molecules is as follows:



where DHP and MHP^- represent the 1,4 DHP molecule and the corresponding anion. Thus, superoxide anion acts as a Brønsted base, deprotonating the 1,4-DHP, and 1,4-DHP acts by scavenging $O_2^{\bullet-}$. The reaction is followed by a series of other chemical reactions that finally produce the complete aromatization of the 1,4-DHP, i.e., the corresponding pyridine derivative, as has been shown recently [10]:



Using the SECM theory developed for a second order homogeneous chemical reaction [12], we can estimate a

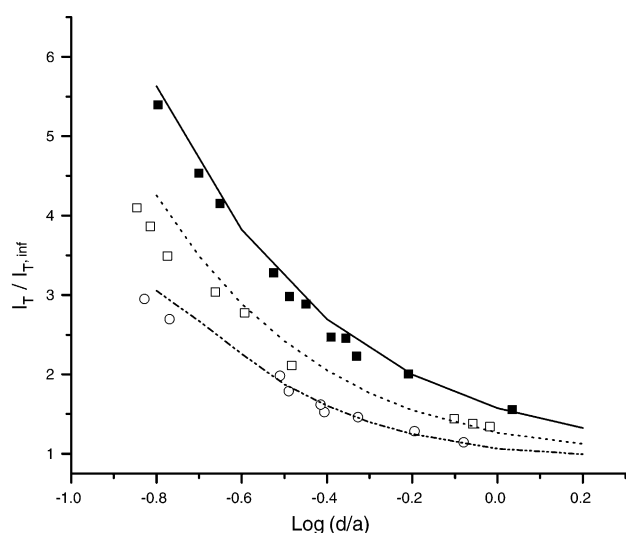


Fig. 8. Normalized tip (feedback) current–distance curves for $[O_2] = 2.1$ mM in the presence of different concentrations of nicardipine, 0 mM (\blacksquare), 5 mM (\square) and 10 mM (\circ), with the theoretical curves described for $K = 0$ (solid line), 1 (dotted line) and 3 (dash-dotted line) ($K = k_i D/a^2$).

Table 1

Interaction constant values k_i calculated by SECM, using the second order homogeneous chemical reaction theory

1,4-DHP	$10^{-5}k_i$ ($M^{-1} s^{-1}$)
Furnidipine	0.9 ± 0.2
Nifedipine	1.9 ± 0.7
Nisoldipine	1.4 ± 0.6
Nicardipine	2.0 ± 0.2
Nimodipine	1.2 ± 0.1
Amlodipine	1.5 ± 0.5
Felodipine	1.2 ± 0.4
CDA-50113	1.1 ± 0.5

value for the chemical interaction constant between superoxide and the 1,4-DHPs (Eq. (6)). Fig. 8 shows the normalized tip (feedback) current–distance curves for $[O_2] = 2.1$ mM (\circ), in the presence of different concentrations of nicardipine with the theoretical curves described for $K = 0, 1$ and 3 ($K = k_i D/a^2$).

According to this theoretical fit, the calculated interaction constants for the different 1,4-DHPs are shown in Table 1. From these values, it is possible to conclude that all the 1,4-DHPs react with superoxide with high interaction constants ($\sim 10^5 M^{-1} s^{-1}$) and no differences between the different 1,4-DHP molecules were found.

4. Conclusions

The $O_2/O_2^{\bullet-}$ redox couple in aprotic medium has been investigated by scanning electrochemical microscopy (SECM). The results showed that the normalized tip experimental current for the $O_2/O_2^{\bullet-}$ couple follows the predicted behavior for a simple diffusion-controlled feedback, i.e., E process. These results are contrary to those previously described by cyclic voltammetry, where a DISP 2 mechanism was proposed.

The experimental conditions mimicked the possible interaction between superoxide and 1,4-DHP in cellular membranes. In fact, there is some evidence revealing that long term administration of a calcium antagonist (1,4-DHP) would result in its accumulation in cellular membranes at concentrations that exceed plasma drug levels by as much as several orders of magnitude [30–32]. Consequently, the use of high concentrations of the drug and the non-aqueous medium resembles in some way both the lipophilic environment and the drug concentrations which are found in biological membranes.

Furthermore, the results of SECM measurements reported in this paper provide a direct method to study the interaction between superoxide and different molecules, since the mechanism of $O_2/O_2^{\bullet-}$ is not complicated by coupled chemical reactions.

In conclusion, this study has demonstrated that SECM can be a useful alternative technique for

electrochemical kinetic studies involving superoxide radical anion.

Acknowledgements

Financial support from FONDECYT (Grant No. 8000016) and University of Chile is gratefully acknowledged.

References

- [1] D.L. Maricle, W.G. Hodgson, *Anal. Chem.* 37 (1965) 1562.
- [2] M.E. Peover, B.S. White, *Electrochim. Acta.* 11 (1966) 1061.
- [3] D.T. Sawyer, J.L. Roberts, *J. Electroanal. Chem.* 12 (1966) 90.
- [4] E.C. Johnson, K.H. Pool, R.E. Hamm, *Anal. Chem.* 39 (1967) 888.
- [5] T. Sraki, H. Kitaoka, *Chem. Pharm. Bull.* 49 (2001) 943.
- [6] M.E. Ortiz, L.J. Núñez-Vergara, J.A. Squella, *J. Electroanal. Chem.* 519 (2002) 46.
- [7] R. Webster, A. Bond, *J. Chem. Soc., Perkin Trans. 2* (1997) 1075.
- [8] T. Okayama, T. Ohsaka, *Electrochim. Acta* 47 (2002) 1561.
- [9] C.M. Collins, C. Sotiriou-Leventis, M.T. Canals, N. Leventis, *Electrochim. Acta* 45 (2000) 2049.
- [10] M.E. Ortiz, L.J. Núñez-Vergara, C. Camargo, J.A. Squella, *Pharm. Res.* 21 (2004) 428.
- [11] P.R. Unwin, A.J. Bard, *J. Phys. Chem.* 95 (1991) 7814.
- [12] F. Zhou, P.R. Unwin, A.J. Bard, *J. Phys. Chem.* 96 (1992) 4917.
- [13] D.A. Treichel, M.V. Mirkin, A.J. Bard, *J. Phys. Chem.* 98 (1994) 5751.
- [14] F. Zhou, A.J. Bard, *J. Am. Chem. Soc.* 116 (1994) 393.
- [15] C. Demaille, P. Unwin, A.J. Bard, *J. Phys. Chem.* 100 (1996) 14137.
- [16] M.V. Mirkin, B.R. Horrocks, *Anal. Chim. Acta* 406 (2000) 119.
- [17] R. Arudi, O. Allen, R. Bielski, *FEBS Lett.* 135 (1981) 265.
- [18] J. Zhang, W. Pietro, A. Lever, *J. Electroanal. Chem.* 403 (1996) 93.
- [19] M.V. Mirkin, F.F. Fan, A.J. Bard, *J. Electroanal. Chem.* 328 (1992) 47.
- [20] A.J. Bard, M.V. Mirkin, P.R. Unwin, D.O. Wipf, *J. Phys. Chem.* 96 (1992) 1861.
- [21] M. Tsionsky, A.J. Bard, M.V. Mirkin, *J. Phys. Chem.* 100 (1996) 17881.
- [22] J. Zhang, P.R. Unwin, *J. Phys. Chem. B* 104 (2000) 2341.
- [23] J. Zhang, C.J. Slevin, P.R. Unwin, *Chem. Commun.* (1999) 1501.
- [24] C.J. Slevin, P.R. Unwin, *Langmuir* 15 (1999) 7361.
- [25] A.L. Barker, P.R. Unwin, S. Amemiya, J.F. Zhou, A.J. Bard, *J. Phys. Chem. B* 103 (1999) 7260.
- [26] M.E. Ortiz, L.J. Núñez-Vergara, J.A. Squella, *J. Electroanal. Chem.* 519 (2002) 46.
- [27] C.M. Collins, *Electrochim. Acta* 45 (2000) 2049.
- [28] S. Bollo, L.J. Núñez-Vergara, J.A. Squella, *J. Electrochem. Soc.* 151 (2004) E322.
- [29] M.E. Ortiz, L.J. Núñez-Vergara, J.A. Squella, *J. Electroanal. Chem.* 549 (2003) 157.
- [30] R.P. Mason, I. Tong, M.W. Trumbore, P.E. Mason, *Am. J. Cardiol.* 84 (4A) (1999) 16L.
- [31] R.P. Mason, S. Campbell, S. Wang, L.G. Hervette, *Mol. Pharmacol.* 36 (1989) 634.
- [32] R.P. Mason, D.E. Moisey, L. Shajenko, *Mol. Pharmacol.* 41 (1992) 315.